

# Location-weighted versus Volume-weighted Mismatch at MRI for Response to Mechanical Thrombectomy in Acute Stroke

Hikaru Fukutomi, MD, PhD • Takayuki Yamamoto, MD, PhD • Igor Sibon, MD, PhD • Soren Christensen, PhD • Nicolas Raposo, MD, PhD • Gaultier Marnat, MD • Jean-François Albucher, MD • Stéphane Olindo, MD • Lionel Calvière, MD • Sharmila Sagnier, MD, PhD • Alain Viguier, MD • Pauline Renou, MD • Adrien Guenego, MD • Mathilde Poli, MD • Jean Darcourt, MD • Sabrina Debruxelles, MD • Amel Drif, BA • Claire Thalamas, MD • Agnès Sommet, MD • Vanessa Rousseau, PhD • Mikael Mazighi, MD, PhD • Fabrice Bonneville, MD, PhD • Gregory W. Albers, MD, PhD • Christophe Cognard, MD, PhD • Vincent Dousset, MD, PhD • Jean Marc Olivot, MD, PhD • Thomas Tourdias, MD, PhD • on behalf of the BBS and FRAME investigators<sup>1</sup>



From the Institut de Bio-Imagerie IBIO (H.F., T.Y., V.D., T.T.), CNRS, UMR-5287 (I.S., S.S.), and INSERM, Neurocentre Magendie, U1215 (V.D., T.T.), Université Bordeaux, 146 rue Léo Saignat, F-33000 Bordeaux Cedex, France; Unité Neurovasculaire (I.S., S.O., S.S., P.R., M.P., S.D.) and Neuroimagerie Diagnostique et Thérapeutique (G.M., V.D., T.T.), CHU de Bordeaux, Bordeaux, France; Stanford Stroke Center, Stanford University, Stanford, Calif (S.C., G.W.A.); Unité Neurovasculaire (N.R., J.F.A., L.C., A.V., J.M.O.), Service de Neuroradiologie (A.G., J.D., F.B., C.C.), and Centre d'Investigation Clinique (A.D., C.T., A.S., V.R.), CHU de Toulouse, Toulouse, France; and Fondation Ophtalmologique Adolphe de Rothschild, Paris, France (M.M.). Received January 10, 2022; revision requested March 15; revision received July 6; accepted August 16. **Address correspondence to T.T.** (email: [thomas.tourdias@chu-bordeaux.fr](mailto:thomas.tourdias@chu-bordeaux.fr)).

This study was supported by public grants from the French Agence Nationale de la Recherche within the context of the Investments for the Future Program (ANR-10-LABX-57) and named Translational Research and Advanced Imaging Laboratory. The brain before stroke study (data set 1) was funded by a public grant from the French government (PHRC programme hospitalier de recherche clinique inter-régional) in 2012. The French acute multimodal imaging to select patients for mechanical thrombectomy study (data set 2) was supported by a research grant from the French Ministry of Health, Clinical Research Hospital Program 2015 (PHRCI-15-076).

<sup>1</sup>BBS and FRAME investigators are listed at the end of this article.

Conflicts of interest are listed at the end of this article.

See also the editorial by Nael in this issue.

Radiology 2023; 306(2):e220080 • <https://doi.org/10.1148/radiol.220080> • Content codes:  

**Background:** A target mismatch profile can identify good clinical response to recanalization after acute ischemic stroke, but does not consider region specificities.

**Purpose:** To test whether location-weighted infarction core and mismatch, determined from diffusion and perfusion MRI performed in patients with acute stroke, could improve prediction of good clinical response to mechanical thrombectomy compared with a target mismatch profile.

**Materials and Methods:** In this secondary analysis, two prospectively collected independent stroke data sets (2012–2015 and 2017–2019) were analyzed. From the brain before stroke (BBS) study data (data set 1), an eloquent map was computed through voxel-wise associations between the infarction core (based on diffusion MRI on days 1–3 following stroke) and National Institutes of Health Stroke Scale (NIHSS) score. The French acute multimodal imaging to select patients for mechanical thrombectomy (FRAME) data (data set 2) consisted of large vessel occlusion–related acute ischemic stroke successfully recanalized. From acute MRI studies (performed on arrival, prior to thrombectomy) in data set 2, target mismatch and eloquent (vs noneloquent) infarction core and mismatch were computed from the intersection of diffusion- and perfusion-detected lesions with the coregistered eloquent map. Associations of these imaging metrics with early neurologic improvement were tested in multivariable regression models, and areas under the receiver operating characteristic curve (AUCs) were compared.

**Results:** Data sets 1 and 2 included 321 (median age, 69 years [IQR, 58–80 years]; 207 men) and 173 (median age, 74 years [IQR, 65–82 years]; 90 women) patients, respectively. Eloquent mismatch was positively and independently associated with good clinical response (odds ratio [OR], 1.14; 95% CI: 1.02, 1.27;  $P = .02$ ) and eloquent infarction core was negatively associated with good response (OR, 0.85; 95% CI: 0.77, 0.95;  $P = .004$ ), while noneloquent mismatch was not associated with good response (OR, 1.03; 95% CI: 0.98, 1.07;  $P = .20$ ). Moreover, adding eloquent metrics improved the prediction accuracy (AUC, 0.73; 95% CI: 0.65, 0.81) compared with clinical variables alone (AUC, 0.65; 95% CI: 0.56, 0.73;  $P = .01$ ) or a target mismatch profile (AUC, 0.67; 95% CI: 0.59, 0.76;  $P = .03$ ).

**Conclusion:** Location-weighted infarction core and mismatch on diffusion and perfusion MRI scans improved the identification of patients with acute stroke who would benefit from mechanical thrombectomy compared with the volume-based target mismatch profile.

Clinical trial registration no. NCT03045146

© RSNA, 2022

Online supplemental material is available for this article.

The ischemic penumbra represents tissue with ischemia that is potentially salvageable if successful reperfusion can be obtained, which is the rationale for recanalization procedures in patients with acute stroke (1,2). In

vivo quantification of penumbra, using either CT perfusion or MR diffusion or perfusion mismatch, has facilitated the identification of patients who are likely to respond favorably to revascularization therapy (3). A

This copy is for personal use only. To order printed copies, contact [reprints@rsna.org](mailto:reprints@rsna.org)

## Abbreviations

AUC = area under the receiver operating characteristic curve, BBS = brain before stroke, FRAME = French acute multimodal imaging to select patients for mechanical thrombectomy, NIHSS = National Institutes of Health Stroke Scale, OR = odds ratio

## Summary

A location-weighted mismatch and infarction core model based on diffusion and perfusion MRI improved the identification of patients with acute stroke who would benefit from mechanical thrombectomy.

## Key Results

- In this secondary analysis of two prospectively collected independent data sets of 321 and 173 patients with stroke, mismatch in eloquent location at MRI was positively associated (odds ratio [OR], 1.14;  $P = .02$ ) with early neurologic improvement after successful mechanical thrombectomy, while eloquent infarction core was negatively associated (OR, 0.85;  $P = .004$ ).
- Both location-weighted eloquent mismatch and infarction core improved good response prediction compared with clinical predictors alone (area under the receiver operating characteristic curve [AUC], 0.73 vs 0.65;  $P = .01$ ) and the volume-based target mismatch profile (AUC, 0.67;  $P = .03$ ).

target mismatch profile is now being used to identify candidates for intravenous thrombolysis (4) or mechanical thrombectomy (5) in an extended time window. Even within the first 6 hours, patients with a target mismatch profile are more likely to recover after mechanical thrombectomy (6). Likewise, the largest treatment effect has been observed in the randomized controlled trials that selected patients based on target mismatch (7) compared with those that did not use perfusion as an inclusion criterion (8). The mismatch concept could even help extend the indications of recanalization to specific conditions, including strokes with a large core volume (9), distal occlusions (10), or very late presentations (11). However, a target mismatch profile treats all brain areas equally even though brain functions differ regionally.

Indeed, several studies have demonstrated that the specific locations of irreversible infarcts, as assessed by follow-up diffusion MRI, were associated with clinical outcome, including modified

Rankin Scale score, cognitive function, spatial neglect, motor function, or impairment of speech (12–19). By transposing the relevance of topography to the penumbra, we could presume that a small volume of penumbra located within an eloquent area could lead to significant clinical recovery after successful reperfusion, while a larger volume of penumbra within a noneloquent area might not impact the outcome. This concept is supported by a recent study (20) that has not yet standardized the measurement of eloquence and was limited to a specific group of patients with a large infarction core volume.

Based on these considerations, penumbra and infarction core “location” could improve identification of good clinical response to recanalization strategies compared with the “volume” approach of the conventional mismatch profile. To test this concept, we rigorously mapped the eloquent brain areas by using an initial large data set of patients with stroke (21). Then, in a second independent stroke data set (6), we used such a map to quantify the eloquent infarction core and mismatch (ie, estimated penumbra), whose predictive values were compared with the standard volume-based mismatch profile. Thus, our aim was to test whether location-weighted infarction core and mismatch from diffusion and perfusion MRI of patients with acute stroke could improve prediction of good response to thrombectomy compared with the target mismatch profile.

## Materials and Methods

### Patients

This is a secondary analysis based on a combination of two prospective studies approved by the institutional ethics committee, the primary objectives of which were unrelated to the present article; these are (a) the brain before stroke (BBS) study (21) that we refer to as data set 1 and (b) the French acute multimodal imaging to select patients for mechanical thrombectomy (FRAME) study (6) that we refer to as data set 2. Inclusion and exclusion criteria are summarized in Table 1.

The BBS study prospectively recruited 428 participants with suspected ischemic stroke from June 2012 to February

**Table 1: Inclusion and Exclusion Criteria of the BBS (Data Set 1) and FRAME (Data Set 2) Studies**

| Study | Inclusion Criteria  | Exclusion Criteria  |
|-------|---|---|
| BBS   | Older than 18 years with a clinical diagnosis of minor-to-severe supratentorial cerebral infarct (NIHSS scores 1–25) 24–72 hours after onset  | Severe dementia; psychiatric troubles matching axis 1 of the Diagnostic and Statistical Manual of Mental Disorders, fourth edition (42), criteria except for major depression; coma; pregnancy or breastfeeding; prestroke mRS score $\geq 1$ ; infratentorial stroke; contraindications to MRI |
| FRAME | Older than 18 years with DWI/PWI or CT perfusion; mechanical thrombectomy initiated within 6 hours after onset; occlusion of the internal carotid artery or the first or second segment of the middle cerebral artery | Any terminal illness with expected survival less than 1 year; evaluation of multimodal imaging profile for management; estimated prestroke mRS score $> 1$ ; more than $> 90$ minutes delay between imaging and femoral puncture; patients under guardianship or analogous situations           |

Note.—BBS = brain before stroke, DWI = diffusion-weighted imaging, FRAME = French acute multimodal imaging to select patients for mechanical thrombectomy, mRS = modified Rankin Scale, NIHSS = National Institutes of Health Stroke Scale, PWI = perfusion-weighted imaging.

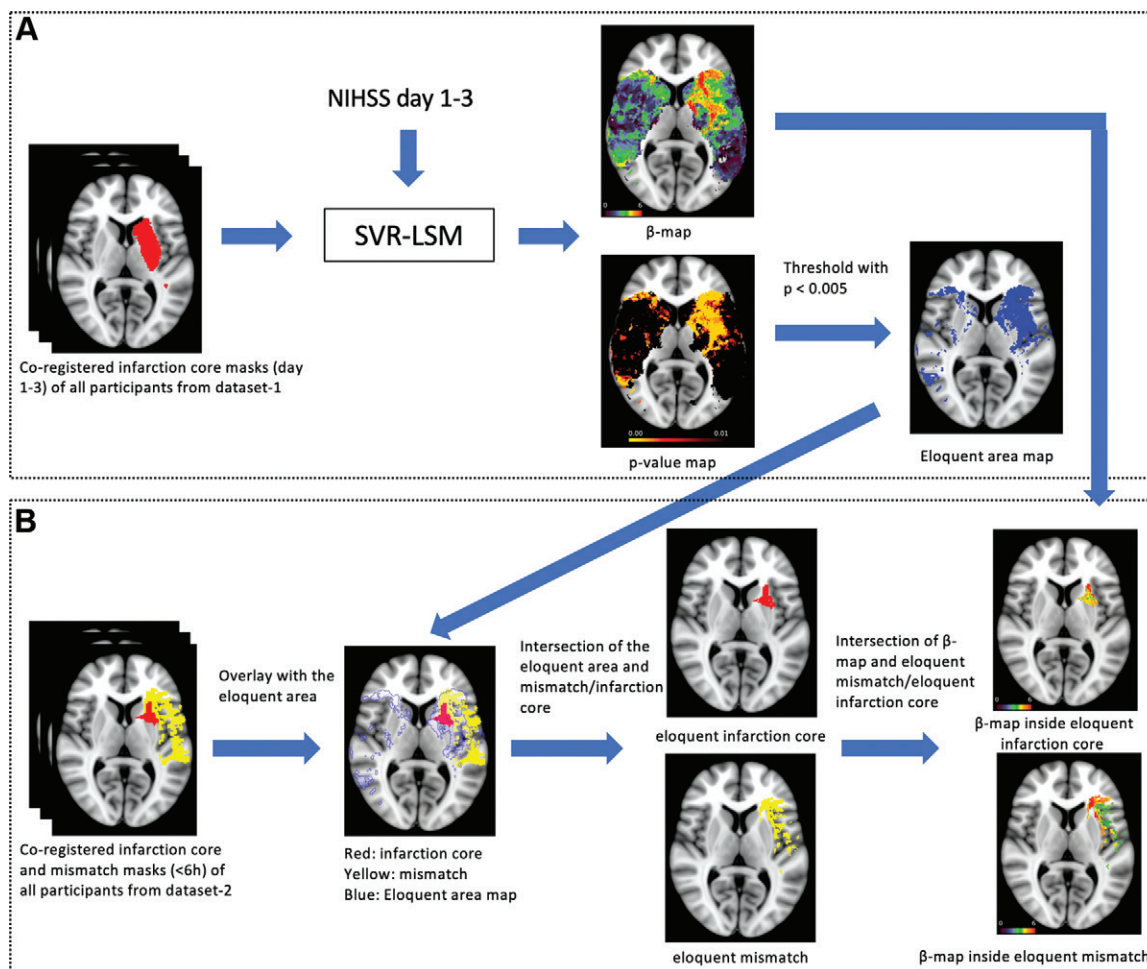


**Figure 1:** (A) Schematic shows the pipeline to estimate the eloquent area map. (B) Schematic shows the pipeline to estimate the sum of  $\beta$  values inside the eloquent mismatch and the sum of  $\beta$  values inside the eloquent infarction core. NIHSS = National Institutes of Health Stroke Scale, SVR-LSM = support vector regression–lesion–symptom mapping.

2015. For data set 1 (BBS), we used diffusion MRI and clinical scores 24–72 hours following onset to map the eloquent brain areas by voxel-wise testing the associations between the final infarction and the National Institutes of Health Stroke Scale (NIHSS) score.

The FRAME study prospectively recruited 218 consecutive participants, from January 2017 to February 2019, who presented with large vessel occlusion–related acute ischemic stroke and underwent acute MRI (performed on arrival) and were subsequently treated with mechanical thrombectomy within the first 6 hours after onset, regardless of the perfusion results (ClinicalTrials.gov no. NCT03045146) (6). We used data set 2 (FRAME) to test the predictive value of standard mismatch (volume-based) versus location-weighted mismatch using the eloquent map from data set 1 (BBS). Because clinical evolution is strongly associated with reperfusion (22,23), we selected only patients who were successfully recanalized, defined by a modified thrombolysis in cerebral infarction score of 2b, 2c, or 3 (86% [187 of 218] of the study sample).

Imaging protocol details are shown in Table S1 (online).

### Estimation of Eloquent Voxels in Data Set 1 (BBS)

Because we aimed to predict good response to recanalization in acute stroke in terms of rapid improvement of the NIHSS score, we first mapped regions associated with higher NIHSS scores if affected by the infarct at postacute MRI (performed between day 1 and day 3 following stroke). For that purpose, infarction masks of data set 1 (BBS) were drawn from diffusion MRI studies and registered to the standard Montreal Neurologic Institute 152 template according to previously described procedures (18). The brain-behavior relation between infarction location and NIHSS score ( $\beta$  map) was estimated with lesion–symptom mapping using support vector regression (24), a multivariate technique that addresses the limitations of conventional mass univariate lesion–symptom mapping techniques (25). The technique has been well validated (26–29) and associates the location of a lesion (infarct) with a clinical score (NIHSS) on a voxel-by-voxel basis, while accounting for intervoxel correlations (24). Only voxels for which at least 10 patients had a lesion were tested. Significant values were obtained using 1000 permutations of the dependent measures. Overall, infarcted voxels associated with a high NIHSS score

within 24–72 hours and a significance threshold of  $P < .005$  were defined as eloquent (Fig 1A).

### Prediction of Good Response after Successful Recanalization in Data Set 2 (FRAME)

**Imaging analysis.**—In data set 2 (FRAME), acute infarction core masks and hypoperfused masks were created from diffusion- and perfusion-weighted images as already described (6,30). The mismatch voxels were those located in the hypoperfused mask but not in the infarction core. Target mismatch was defined according to the EXTEND-IA (Extending the Time for Thrombolysis in Emergency Neurological Deficits–Intra-Arterial) trial threshold (7), with a mismatch ratio greater than 1.2, mismatch volume greater than 10 mL, and ischemic core volume less than 70 mL.

Infarction core and mismatch masks were registered to the standard template using advanced normalization tools (31). Their total volumes were calculated within the template space and then separated as eloquent or noneloquent core and mismatch (whose sum was equivalent to the total volume of each tissue type) based on the intersection with the eloquent map computed from data set 1 (BBS). Then, as each individual voxel was more associated or less associated with the NIHSS score, we took such weight into account by computing the sum of  $\beta$  values within each mask (Fig 1B).

**Clinical definition of outcome.**—Good response was defined as an NIHSS score of 0 or 4-point improvement the day after mechanical thrombectomy because this threshold of early neurologic improvement was found to be the best surrogate for longer-term disability (32,33).

### Statistical Analysis

Baseline characteristics are provided as numbers and percentages or medians with IQRs and were compared between patients with “good” versus “poor” responses by using the  $\chi^2$  test or Wilcoxon Mann-Whitney  $U$  test, as appropriate.

To test the prognostic value of eloquent mismatch, univariable analysis was performed and five multivariable logistic regression models were constructed. Model 1 included prespecified clinical variables with prognostic value based on the literature (34): age, baseline NIHSS score, recombinant tissue-type plasminogen activator, history of diabetes mellitus, systolic blood pressure, and time from onset to the end of mechanical thrombectomy. Model 2 included variables in model 1 plus a target mismatch profile. Model 3 included variables in model 1 plus eloquent mismatch and eloquent infarction core (sum of  $\beta$  values within each mask) instead of target mismatch, while model 4 included variables in model 1 plus noneloquent mismatch and noneloquent infarction core (sum of  $\beta$  values within each mask). Model 5 combined variables in model 1 plus target mismatch, eloquent mismatch, and eloquent infarction core. As a secondary analysis, we also tested these models in patients with a large infarction volume ( $>70$  mL). For internal validation, we used the 10-fold cross-validation procedure to correct the area under the receiver operating characteristic

curve (AUC) of each model. The bootstrap technique with 2000 replications was performed to estimate the two-sided 95% CIs of each AUC. The DeLong test was used for the comparison of AUCs between models. Then, we used the Youden index to find the optimal cutoff and to determine the performance values of location-weighted mismatch, which we compared with those of target mismatch. To check the collinearity among variables, the Spearman correlation test was performed for each combination of quantitative variables. All tests were two sided and a  $P$  value less than .05 was considered indicative of a statistically significant difference. Analyses were conducted using R version 4.0.3 (The R Foundation).

## Results

### Patient Characteristics

Regarding data set 1 (BBS), among the 428 recruited participants with suspected ischemic stroke, 107 were excluded from the analysis for reasons summarized in the flowchart (Fig 2A). Among the 321 included patients, the median age was 69 years (IQR, 58–80 years), the median NIHSS score was 4 (IQR, 2–7), and 207 (64%) were men. Other baseline patient characteristics are shown in Table 2.

Regarding data set 2 (FRAME), among the 218 enrolled participants, 187 underwent successful reperfusion with modified thrombolysis in cerebral infarction scores of 2b, 2c, or 3. Twelve patients who had only CT perfusion studies or inadequate MRI perfusion images were excluded. Two patients without NIHSS scores at day 1 were also excluded. Of the 173 patients included in the analysis, 120 (69%) were classified as having a good response after reperfusion (Fig 2B). The median age was 74 years (IQR, 65–82 years), the median NIHSS score was 17 (IQR, 12–21), and 90 (52%) were women. Other baseline patient characteristics are shown in the first column of Table 3.

### Map of Eloquent Areas in Association with NIHSS Score after Acute Stroke

In patients in data set 1 (BBS), brain areas (voxels) in most of the middle cerebral arterial territory (35) were lesioned in more than 10 patients and could have been included for the lesion-symptom mapping analysis using support vector regression, but some areas of the primary motor cortex (especially territories dedicated to motor functions of hips, legs, and feet, as well as the left hand) were not lesioned in more than 10 patients and, thus, could not be analyzed. We found that, although infarcts were distributed bilaterally and symmetrically and concentrated in the deep gray matter (Fig 3A), the voxels that showed the strongest associations with high NIHSS scores (ie, higher  $\beta$  values) were predominantly located on the left side (Fig 3B). Eloquent voxels, after keeping only those whose associations were significant at the  $P < .005$  threshold, were distributed in the lower part of the bilateral precentral gyrus and corona radiata, dominantly on the left side of the striatum, caudate nucleus, insular cortex, external capsule, and deep white matter (Fig 3C, 3D).



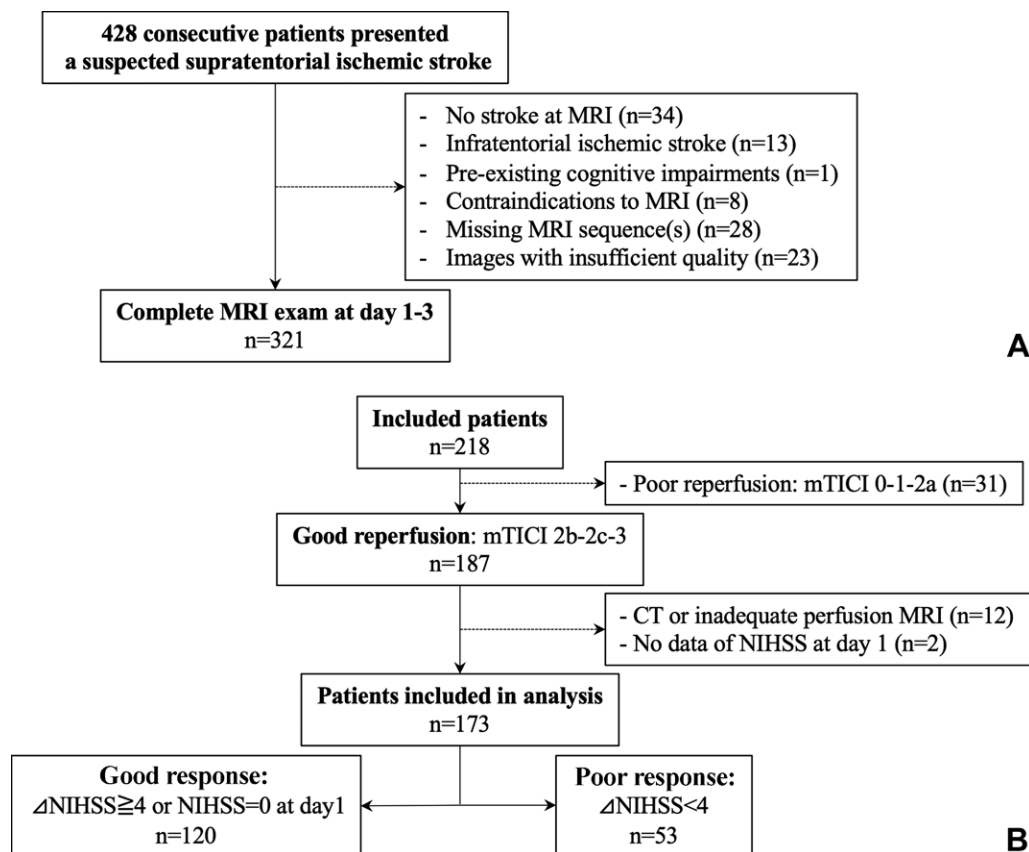


**Figure 2:** Flowcharts of patient inclusion and exclusion for **(A)** data set 1 (brain before stroke) and **(B)** data set 2 (French acute multimodal imaging to select patients for mechanical thrombectomy). NIHSS = National Institutes of Health Stroke Scale, mTICI = modified thrombolysis in cerebral infarction.

**Table 2: Baseline Characteristics of Patients in Data Set 1 (BBS)**

| Variable  | Value (n = 321) |
|---|-----------------|
| Age (y)*  | 69 (58–80)      |
| Sex   |                 |
| M   | 207 (64)        |
| F   | 114 (36)        |
| Hypertension  | 214 (67)        |
| Hypercholesterolemia  | 149 (46)        |
| Diabetes mellitus   | 53 (17)         |
| Active smoking  | 145 (45)        |
| NIHSS score*  | 4 (2–7)         |
| Time from onset to MRI (h)*                                 | 46 (31–58)      |
| Infarction volume (mL)*                                     | 14.4 (2.6–42.0) |
| Recanalization procedure (thrombolysis and/or thrombectomy) | 151 (47)        |

Note.—Except where indicated, data are numbers of patients, with percentages in parentheses. BBS = brain before stroke, NIHSS = National Institutes of Health Stroke Scale.

\* Data are medians, with IQRs in parentheses.

### Penumbra Imaging of Patients with Large Vessel Occlusion–related Acute Ischemic Stroke within the First 6 Hours

In patients in data set 2 (FRAME), both infarction core and mismatch were distributed symmetrically and bilaterally (Fig 4).

Overall, the median volume of the infarction core was 22.0 mL (IQR, 10.2–73.0 mL), and the median volume of mismatch was 91.6 mL (IQR, 53.9–133.0 mL), resulting in 76% (132 of 173) of patients fulfilling the criteria of target mismatch (Table 3). The intersection of these volumes with the eloquent map described in the previous paragraph showed that the median volume of eloquent mismatch was 17.8 mL (IQR, 9.6–25.1 mL), which was 19.4% (17.8 of 91.6) of the total mismatch, while the remaining 75.6 mL (IQR, 42.4–101.4 mL) involved less eloquent voxels. Therefore, both the volume-based infarction core and mismatch, as well as the location-weighted infarction core and mismatch, could be assessed individually and provided different quantifications.

### Prediction of Good Response to Recanalization

In data set 2 (FRAME), patients with a good response to mechanical thrombectomy were less likely to have diabetes (12% vs 26%,  $P = .03$ ), had lower systolic blood pressure (median, 145 mm Hg vs 160 mm Hg;  $P < .001$ ), and were more likely to have received recombinant tissue-type plasminogen activator in addition to the mechanical thrombectomy procedure (76% vs 57%,  $P = .02$ ) compared with patients with a poor response (Table 3). In terms of the imaging profile, those with a good response had more target mismatch (82% vs 62%,  $P = .007$ ), which corresponded to a smaller infarction core volume (median, 18.0 mL

**Table 3: Baseline Characteristics of Patients in Data Set 2 (FRAME)**

| Variable   | All Patients<br>(n = 173) | Good Response<br>Group (n = 120) | Poor Response<br>Group (n = 53) | P Value |
|--|---------------------------|----------------------------------|---------------------------------|---------|
| <b>Clinical</b>  |                           |                                  |                                 |         |
| Age (y)  | 74 (65–82)                | 73 (64–82)                       | 76 (70–83)                      | .15*    |
| Sex†   |                           |                                  |                                 |         |
| F  | 90 (52)                   | 60 (50)                          | 30 (57)                         | .52‡    |
| M  | 83 (48)                   | 60 (50)                          | 23 (43)                         |         |
| Hypertension†  | 101 (58)                  | 71 (59)                          | 30 (57)                         | .88‡    |
| Hypercholesteremia†  | 47 (27)                   | 34 (28)                          | 13 (25)                         | .74‡    |
| Diabetes mellitus†   | 28 (16)                   | 14 (12)                          | 14 (26)                         | .03‡§   |
| Active smoking†  | 26 (15)                   | 15 (13)                          | 11 (21)                         | .24‡    |
| Baseline NIHSS score   | 17 (12–21)                | 16 (12–20)                       | 19 (10–24)                      | .46*    |
| Blood glucose level (mM)   | 6.6 (5.8–7.7)             | 6.5 (5.6–7.4)                    | 7.0 (6.4–8.5)                   | .004§   |
| Internal carotid artery occlusion†                                     | 20 (12)                   | 13 (11)                          | 7 (13)                          | .85‡    |
| <b>Thrombectomy and thrombolysis</b>                                   |                           |                                  |                                 |         |
| rtPA†  | 121 (70)                  | 91 (76)                          | 30 (57)                         | .02‡§   |
| Time from stroke onset to end of MT procedure (min)                    | 256 (207–336)             | 252 (205–318)                    | 291 (209–364)                   | .13*    |
| General anesthesia†  | 71 (41)                   | 45 (38)                          | 26 (49)                         | .21‡    |
| SBP at arrival in the catheterization laboratory (mm Hg)               | 150 (135–170)             | 145 (130–160)                    | 160 (145–176)                   | <.001*  |
| <b>Imaging (diffusion and perfusion MRI)</b>                           |                           |                                  |                                 |         |
| Target mismatch†   | 132 (76)                  | 99 (82)                          | 33 (62)                         | .007‡§  |
| <b>Core</b>  |                           |                                  |                                 |         |
| Volume of infarction core (mL)   | 22.0 (10.2–73.0)          | 18.0 (8.7–52.9)                  | 44.9 (18.1–128.0)               | .001*§  |
| Volume of eloquent infarction core (mL)                                | 5.5 (2.3–17.4)            | 5.1 (2.0–13.1)                   | 15.7 (2.7–29.9)                 | .006*§  |
| Volume of noneloquent infarction core (mL)                             | 15.1 (5.7–58.0)           | 10.9 (4.8–33.0)                  | 21.9 (14.4–99.5)                | .001*§  |
| Sum of $\beta$ values in eloquent infarction core ( $\times 10^3$ )    | 18.7 (7.7–59.2)           | 17.6 (6.8–44.3)                  | 52.5 (9.2–100.5)                | .006*§  |
| Sum of $\beta$ values in noneloquent infarction core ( $\times 10^3$ ) | 42.8 (14.6–130.0)         | 28.9 (11.8–89.0)                 | 64.9 (39.4–206.2)               | .002*§  |
| <b>Mismatch</b>  |                           |                                  |                                 |         |
| Volume of mismatch (mL)  | 91.6 (53.9–133.0)         | 96.4 (60.7–135.6)                | 81.8 (44.2–116.7)               | .08*    |
| Volume of eloquent mismatch (mL)                                       | 17.8 (9.6–25.1)           | 19.1 (11.7–27.4)                 | 11.8 (4.7–20.9)                 | <.001*  |
| Volume of noneloquent mismatch (mL)                                    | 75.6 (42.4–101.4)         | 78.7 (46.0–105.6)                | 68.3 (34.3–95.6)                | .19*    |
| Sum of $\beta$ values in eloquent mismatch ( $\times 10^3$ )           | 60.7 (33.0–85.8)          | 65.4 (40.5–92.9)                 | 40.0 (16.1–71.8)                | <.001*  |
| Sum of $\beta$ values in noneloquent mismatch ( $\times 10^3$ )        | 158.6 (92.9–225.3)        | 161.9 (105.0–234.5)              | 148.2 (55.3–206.8)              | .049*§  |

Note.—Except where indicated, data are medians, with IQRs in parentheses. FRAME = French acute multimodal imaging to select patients for mechanical thrombectomy, MT = mechanical thrombectomy, NIHSS = National Institutes of Health Stroke Scale, rtPA = recombinant tissue-type plasminogen activator, SBP = systolic blood pressure.

\* Wilcoxon Mann-Whitney *U* test.

† Data are numbers of patients, with percentages in parentheses.

‡  $\chi^2$  test.

§  $P < .05$  indicates statistical significance.

||  $P < .001$  indicates statistical significance.

[IQR, 8.7–52.9 mL] vs 44.9 mL [IQR, 18.1–128.0 mL];  $P = .001$ ), but we found no evidence of a larger volume of mismatch (median, 96.4 mL [IQR, 60.7–135.6 mL] vs 81.8 mL [IQR, 44.2–116.7 mL];  $P = .08$ ). Interestingly, when considering location-weighted metrics rather than raw volumes, patients with a good response had larger volumes of eloquent mismatch (median, 19.1 mL [IQR, 11.7–27.4 mL] vs 11.8 mL [IQR, 4.7–20.9 mL];  $P < .001$ ) but no difference in volumes of noneloquent mismatch (median, 78.7 mL [IQR, 46.0–105.6 mL] vs 68.3 mL [IQR, 34.3–95.6 mL];  $P = .19$ ) compared with those with a poor response. These results support the concept that when salvageable tissue in-

volves clinically relevant (eloquent) regions, a larger increase in NIHSS score is expected. The same was true when considering sums of  $\beta$  values that account for the individual weights of each voxel. In contrast, a larger volume of infarction core, which is supposed to be irreversible (or poorly reversible), was always associated with a poor response regardless of its location (Table 3).

In the primary multivariable analyses (Table 4), a volume-based profile of target mismatch was associated with good clinical response (odds ratio [OR], 3.37; 95% CI: 1.36, 8.34;  $P = .009$  in model 2) independent of the prespecified clinical predictors (model 1). When replacing target mismatch

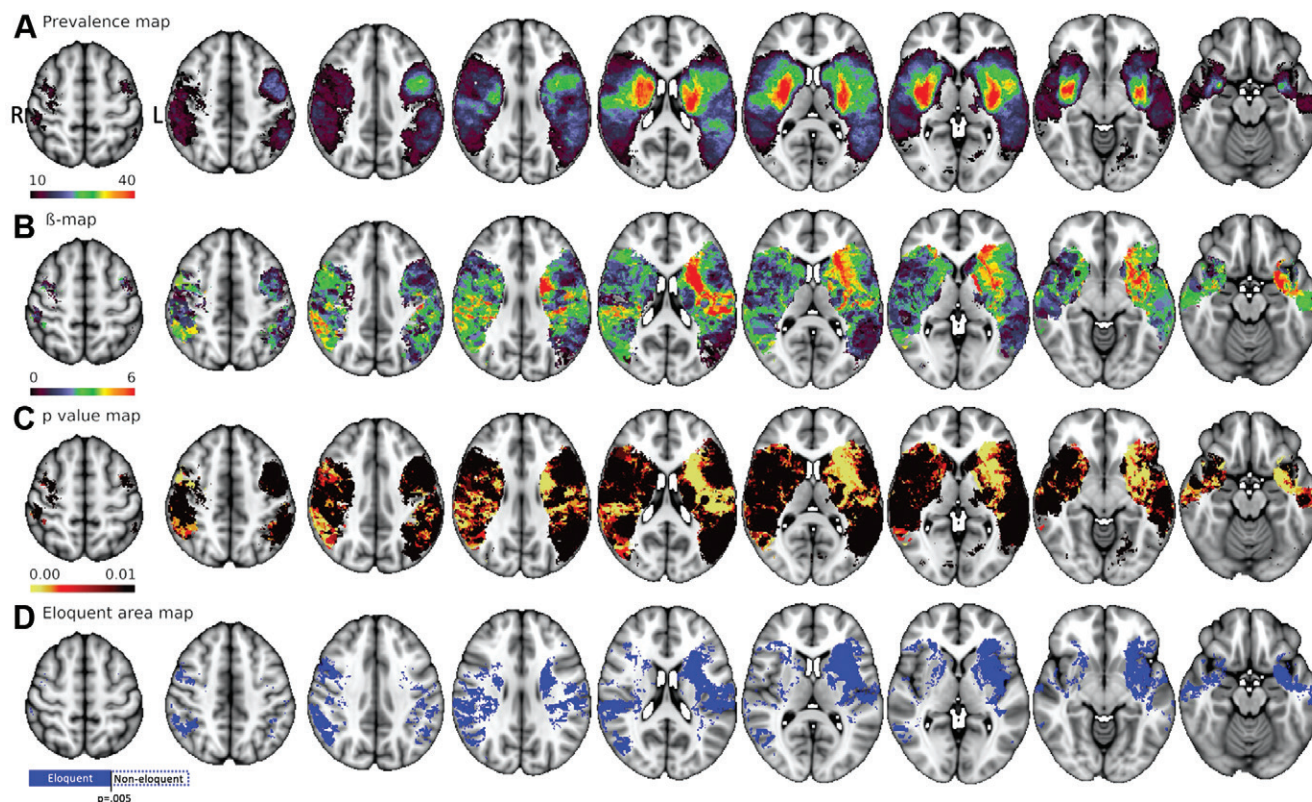


**Figure 3:** Maps for data set 1 (brain before stroke). **(A)** Prevalence map shows infarction core. Only voxels for which more than 10 patients had a lesion were represented and included in the lesion-symptom mapping using support vector regression. **(B)**  $\beta$  map shows lesion-symptom relations between infarction and the National Institutes of Health Stroke Scale score calculated from lesion-symptom mapping using support vector regression. **(C)**  $P$  value map. **(D)** Eloquent area map, defined after thresholding the  $P$  value map at  $P < .005$ . L = left, R = right.

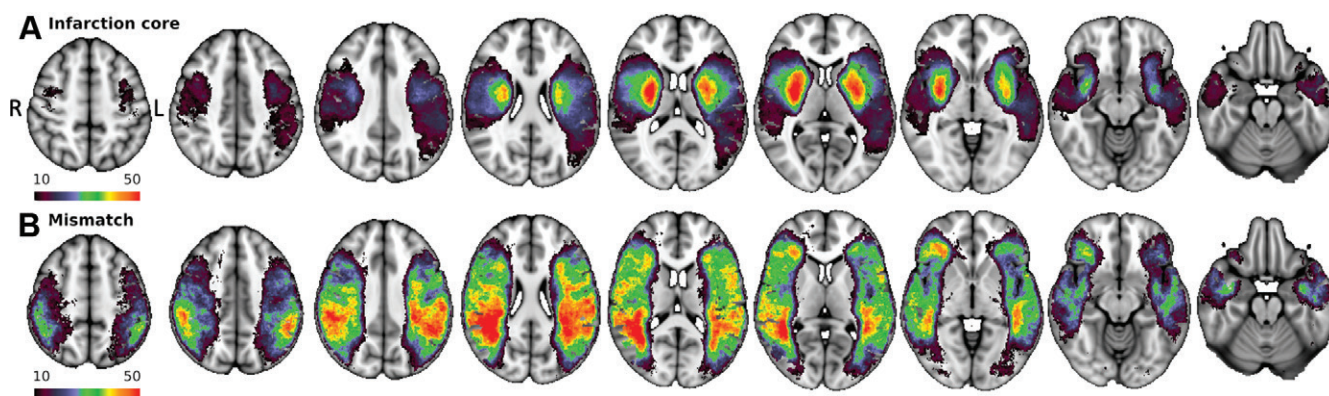


**Figure 4:** Prevalence maps of **(A)** infarction core and **(B)** mismatch in patients in data set 2 (French acute multimodal imaging to select patients for mechanical thrombectomy) show symmetrical and bilateral distribution. L = left, R = right.

by location-weighted metrics (model 3), more eloquent mismatch (sum of  $\beta$  values) was independently and positively associated with a good response (OR, 1.14; 95% CI: 1.02, 1.27;  $P = .02$ ), while more eloquent infarction core (sum of  $\beta$  values) was negatively associated with a good response (OR, 0.85; 95% CI: 0.77, 0.95;  $P = .004$ ). As a negative control condition, we found no evidence of an association between noneloquent mismatch and good clinical response (OR, 1.03; 95% CI: 0.98, 1.07;  $P = .20$ ). The strength of association for

the noneloquent infarction core was reduced compared with eloquent voxels but was still significant (OR, 0.95; 95% CI: 0.92, 0.997;  $P = .03$ ), probably because voxels dichotomized as noneloquent (with significance set at  $P < .005$ ) could still convey some clinical functions as captured by the NIHSS. As another control, we combined the volume-based metric (target mismatch) and location-weighted metrics; only the latter remained significantly and independently associated with good clinical response (model 5).



**Table 4: Logistic Regression Models for Prediction of Early Neurologic Improvement**

| Variable   | Odds Ratio         | P Value            |
|--|--------------------|--------------------|
| <b>Univariable Analysis</b>  |                    |                    |
| Age (+5 y)   | 0.92 (0.81, 1.04)  | .18                |
| Onset to end of MT (+10 min)   | 0.97 (0.94, 1.01)  | .12                |
| rtPA (yes)   | 2.71 (1.35, 5.47)  | .005*              |
| Baseline NIHSS score (+1 point)  | 0.99 (0.94, 1.04)  | .59                |
| Diabetes mellitus  | 0.35 (0.15, 0.8)   | .01                |
| SBP at arrival of MT (+1 mm Hg)  | 0.82 (0.72, 0.94)  | .003 <sup>†</sup>  |
| Sum of $\beta$ values in eloquent infarction core (+10 000)  | 0.87 (0.81, 0.94)  | <.001 <sup>†</sup> |
| Sum of $\beta$ values in eloquent mismatch (+10 000)   | 1.19 (1.08, 1.32)  | <.001 <sup>†</sup> |
| Sum of $\beta$ values in noneloquent infarction core (+10 000)                                       | 0.95 (0.92, 0.98)  | .003 <sup>†</sup>  |
| Sum of $\beta$ values in noneloquent infarction penumbra (+10 000)                                   | 1.04 (1, 1.08)     | .046*              |
| <b>Multivariable analysis</b>  |                    |                    |
| <b>Model 1: clinical variables</b>   |                    |                    |
| rtPA (yes)   | 2.20 (1.04, 4.68)  | .04*               |
| Diabetes mellitus  | 0.36 (0.14, 0.88)  | .03*               |
| SBP at arrival of MT (+1 mm Hg)  | 0.83 (0.72, 0.96)  | .01*               |
| <b>Model 2: clinical variables and target mismatch</b>   |                    |                    |
| Diabetes mellitus  | 0.35 (0.14, 0.89)  | .03*               |
| SBP at arrival of MT (+1 mm Hg)  | 0.85 (0.73, 0.98)  | .03*               |
| Target mismatch (yes)  | 3.37 (1.36, 8.34)  | .009*              |
| <b>Model 3: clinical variables, eloquent mismatch, and eloquent infarction core</b>                  |                    |                    |
| SBP at arrival of MT (+1 mm Hg)  | 0.82 (0.69, 0.97)  | .02*               |
| Sum of $\beta$ values in eloquent infarction core (+10 000)  | 0.85 (0.77, 0.95)  | .004 <sup>†</sup>  |
| Sum of $\beta$ values in eloquent mismatch (+10 000)   | 1.14 (1.02, 1.27)  | .02*               |
| <b>Model 4: clinical variables, noneloquent mismatch, and noneloquent infarction core</b>            |                    |                    |
| SBP at arrival of MT (+1 mm Hg)  | 0.84 (0.72, 0.98)  | .03*               |
| Sum of $\beta$ values in noneloquent infarction core (+10 000)                                       | 0.95 (0.92, 0.997) | .03*               |
| Sum of $\beta$ values in noneloquent infarction penumbra (+10 000)                                   | 1.03 (0.98, 1.07)  | .20                |
| <b>Model 5: clinical variables, target mismatch, eloquent mismatch, and eloquent infarction core</b> |                    |                    |
| Baseline NIHSS score (+1 point)  | 1.08 (1.00, 1.17)  | .047*              |
| SBP at arrival of MT (+1 mm Hg)  | 0.81 (0.69, 0.96)  | .02*               |
| Target mismatch (yes)  | 0.64 (0.17, 2.43)  | .51                |
| Sum of $\beta$ values in eloquent infarction core (+10 000)  | 0.83 (0.72, 0.95)  | .01*               |
| Sum of $\beta$ values in eloquent penumbra (+10 000)   | 1.15 (1.03, 1.29)  | .02*               |

Note.—Data in parentheses are 95% CIs. In multivariable analysis, location-based metrics and only variables significantly associated were shown. MT = mechanical thrombectomy, NIHSS = National Institutes of Health Stroke Scale, rtPA = recombinant tissue-type plasminogen activator, SBP = systolic blood pressure.

\*  $P < .05$  indicates statistical significance.

<sup>†</sup>  $P < .005$  indicates statistical significance.

In terms of predictive performance (Fig 5), we found no evidence of a difference in AUC values between model 1 and model 2 with target mismatch (AUC, 0.65 [95% CI: 0.56, 0.73] vs 0.67 [95% CI: 0.59, 0.76];  $P = .27$ ), while adding the location-weighted metrics in model 3 led to a better prediction (AUC, 0.73; 95% CI: 0.65, 0.81) compared with the clinical information alone in model 1 ( $P = .01$ ) and also compared with volume-based target mismatch in model 2 ( $P = .03$ ). We found no evidence that the noneloquent metrics (model 4) changed the predictive performance (AUC, 0.66; 95% CI: 0.57, 0.75;  $P = .68$  vs model 1 and  $P = .39$  vs model 2) (Fig 5). By using  $36.3 \times 10^3$  as a cutoff for the sum of  $\beta$  values to dichotomize a significant versus nonsignificant amount

of eloquent mismatch, we showed that we could anticipate good response with a higher positive predictive value, negative predictive value, and specificity compared with the target mismatch definition (Fig 6, Table 5).

#### Subgroup Analysis of Patients with a Large Infarction Core Volume (>70 mL)

In our subgroup analysis of 36 patients who had a large infarction core volume (>70 mL), location-weighted metrics could not improve the identification of good response compared with clinical information (AUC, 0.71 [95% CI: 0.53, 0.87] in model 1 vs 0.75 [95% CI: 0.57, 0.90] in model 3;  $P = .83$ ), which could be due to small sample size.



### Collinearity

In all the above analyses, the highest correlation coefficient was  $r$  of 0.59 (ie,  $<0.8$ ) (Fig S1 [online]), which is an acceptable level of collinearity according to thresholds from the literature (36).

### Discussion

Whether location-weighted mismatch could identify patients with better responses following mechanical thrombectomy

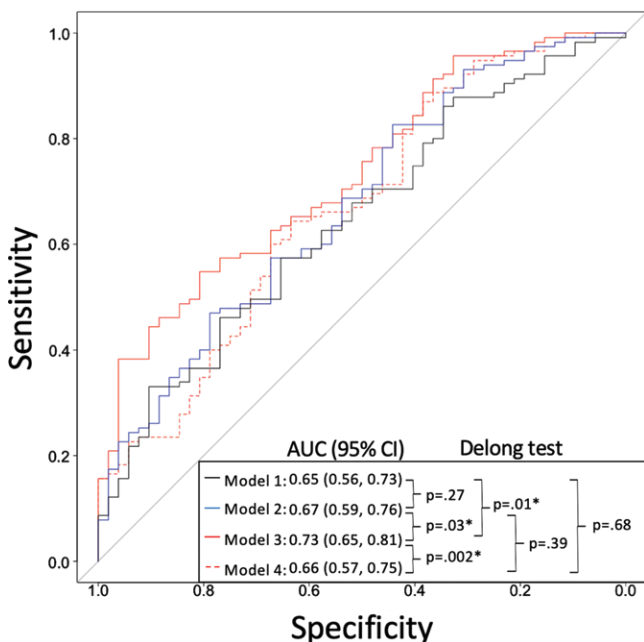


**Figure 5:** Receiver operating characteristic curves show the areas under the receiver operating characteristic curve (AUCs) with 95% CIs for the logistic regression models. Model 1 included only clinical variables, model 2 included clinical variables plus target mismatch, model 3 included clinical variables plus eloquent location-weighted metrics (sum of  $\beta$  values), and model 4 included clinical variables plus noneloquent location-weighted metrics (sum of  $\beta$  values). The DeLong test was used for comparison of AUCs between models. The AUC of model 3 was significantly higher than those of models 1, 2, and 4, while the AUC of model 4 was not significantly higher than those of models 1 and 2. \*  $P < .05$  indicates statistical significance.

has not been fully investigated, even though brain functions differ regionally. In our study, by combining a whole-brain eloquence map with mismatch profiles of patients successfully recanalized, the models showed that eloquent mismatch and eloquent infarction core were associated with improvement of NIHSS scores (odds ratio, 1.14 [ $P = .02$ ] and 0.85 [ $P = .004$ ], respectively), which translated into modest improvement in prediction of good response (area under the receiver operating characteristic curve [AUC], 0.73) compared with clinical predictors (AUC, 0.65;  $P = .01$ ) and conventional volume-based mismatch (AUC, 0.67;  $P = .03$ ). The region-specific assessment may contribute to further refinement of the proper management of patients with acute ischemic infarction in the future.

Recanalization following acute stroke can drive clinical recovery through the salvage of penumbra, albeit with an associated risk of hemorrhage. An imaging definition of penumbra is used to select the patients with a favorable benefit-to-risk ratio for recanalization in extended time windows (4,5) or in certain conditions, such as strokes with large core volumes (9) or very late presentations (11). However, volume-based mismatch might be imprecise to predict the chance of a favorable response. In comparison with the relevance of topography that has been well described in irreversible infarcts (12–19), we could anticipate that a small volume of mismatch could be worth rescuing if strongly clinically relevant, while rescuing larger but less eloquent volumes might not impact the outcome. In line with this concept, we have directly highlighted the additional predictive value of location-weighted metrics compared with raw volume-based mismatch profiles because eloquent location-weighted metrics outperformed the standard mismatch definition. It is also interesting to note that the derived noneloquent metrics provided strong negative controls to validate this concept. The relevance of such location-weighted metrics will need to be tested in more patients with larger infarction core volumes ( $>70$  mL) to determine whether it can help to improve the safety of mechanical thrombectomy in this subpopulation (37).

Our results are consistent with a recent study that also pointed to the relevance of location-based mismatch specifically

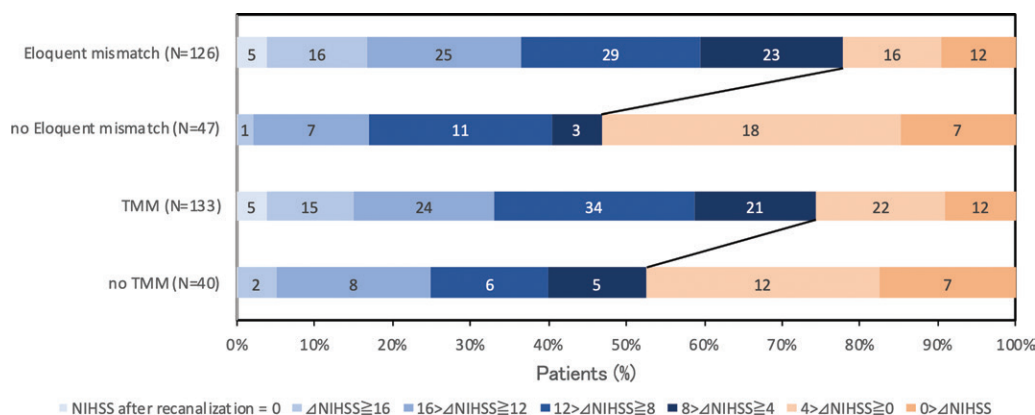


**Figure 6:** Chart shows the variation of clinical deficit after successful recanalization in data set 2 (French acute multimodal imaging to select patients for mechanical thrombectomy, or FRAME) according to the acute imaging profile, dichotomized as eloquent mismatch presence or absence (top rows) or target mismatch (TMM) presence or absence (bottom rows). Differences in the number of patients with early neurologic improvement (blue) between the groups are indicated with the black connecting lines. NIHSS = National Institutes of Health Stroke Scale.

**Table 5: Diagnostic Accuracy Measures in Data Set 2 (FRAME)**

|                   | Clinical Response* |      |       | PPV         | NPV         | Sensitivity | Specificity | Accuracy    |
|-------------------|--------------------|------|-------|-------------|-------------|-------------|-------------|-------------|
|                   | Good               | Poor | Total |             |             |             |             |             |
| Target mismatch   |                    |      |       | 74 (71, 78) | 48 (35, 60) | 83 (78, 87) | 36 (26, 45) | 68 (62, 74) |
| Positive          | 99                 | 34   | 133   | ...         | ...         | ...         | ...         | ...         |
| Negative          | 21                 | 19   | 40    | ...         | ...         | ...         | ...         | ...         |
| Total             | 120                | 53   | 173   | ...         | ...         | ...         | ...         | ...         |
| Eloquent mismatch |                    |      |       | 78 (73, 86) | 53 (42, 64) | 82 (77, 86) | 47 (37, 57) | 71 (65, 77) |
| Positive          | 98                 | 28   | 126   | ...         | ...         | ...         | ...         | ...         |
| Negative          | 22                 | 25   | 47    | ...         | ...         | ...         | ...         | ...         |
| Total             | 120                | 53   | 173   | ...         | ...         | ...         | ...         | ...         |

Note.—Except where indicated, data are percentages, with 95% CIs in parentheses. FRAME = French acute multimodal imaging to select patients for mechanical thrombectomy, NPV = negative predictive value, PPV = positive predictive value.

\* Data are numbers of patients.

in patients with a large infarction core volume (17). Herein, we extended this conclusion to any type of stroke volume. We analyzed a larger group of patients treated with mechanical thrombectomy that was decided when blinded to acute perfusion imaging (6), which strongly reduces potential selection bias. We could also focus on patients known to be successfully recanalized, which is crucial for proper validation, as the direction of the effect is expected to be opposite in patients who have undergone recanalization versus those who have not. We further strengthen this concept because the previous eloquent map was subjectively defined according to the literature with equivalent weight for all eloquent regions (20), while we could objectively define eloquent voxels from a large independent data set and we could even account for the differential weight of each individual voxel. Such an eloquent map showed a reasonable distribution, including the lower part of the precentral gyrus, which is related to motor function, and corona radiata (38), but also predominantly the left language-related areas and left caudate nucleus (39). In the future we could also refine maps for right-handed versus left-handed patients to improve quantification of language-related eloquence.

Our study had several limitations. First, to provide proof-of-concept for such a refined mismatch approach, we “experimentally” focused on variation of clinical deficit after successful recanalization as this is directly driven by the rescued penumbra. Early NIHSS score improvement will be strongly associated with long-term disability (32,33,40), but we could not directly test if location-weighted mismatch predicts long-term disability. Second, voxels for which less than 10 patients had a lesion could not be tested for their associations with NIHSS scores in the lesion-symptom mapping analysis using support vector regression. This was the case for the primary motor cortical areas dedicated to lower extremities and to the left hand that were not included in our eloquent map, although they are clearly eloquent areas. New eloquent maps with a larger number of patients with stroke in these eloquent areas could improve the model performance in the future. Third, the data sets were not originally collected to address this secondary hypothesis and some analyses might be underpowered. Fourth,

the two data sets were noncomparable (smaller infarcts in data set 1 [BBS]). However, the lesion-symptom mapping using support vector regression technique that was used to generate the eloquent map identified individual voxels associated with NIHSS scores while controlling for lesion volume, in contrast to standard voxel-based lesion-symptom mapping approaches (25). Finally, this methodology could be more relevant to apply to CT perfusion, which is performed at the majority of institutions for acute stroke settings; however, a dedicated study will be required to adapt the current methodology to CT perfusion.

In conclusion, although recanalization in ischemic stroke can be decided with only minimal imaging information (41), certain situations already benefit from individual evaluation of the penumbra (4,5) and may extend in the future to offer safe reperfusion therapies for patients with stroke with a large core volume (9), distal occlusions, or very late presentations (11). Herein, we provide proof of concept for a revisited mismatch at diffusion and perfusion MRI that provides integrated location-based classification with the potential to help identify new candidates for reperfusion in the future.

**BBS and FRAME co-investigators:** Louis Fontaine, MD, François Chollet, MD, Marianne Barbieux, MD (Neurology, CHU Toulouse, France); Caterina Michelozzi, MD, Philippe Tall, MD, Anne-Christine Januel (Neuroradiology, CHU Toulouse, France); François Caparros, MD (Neurology, CHU Lille, France); Brigitte Pouzet, PhD, Fabienne Calvas, MD, Monique Galitzki, MD (Clinical Investigation Center, CHU Toulouse, France); François Rouanet, MD, Sylvain Ledure, BA (Neurology, CHU Bordeaux, France); Patrice Ménégon, MD, Jerome Berge, MD, Xavier Barreau, MD, Florent Gariel, MD (Neuroradiology, CHU Bordeaux, France); Julien Asselineau, PhD, Paul Perez, MD (Methodology Department, CHU Bordeaux, France); and Michael Mlynash (Stanford Stroke Center, California, U.S.).

**Author contributions:** Guarantors of integrity of entire study, **G.M., J.F.A., C.T., V.R., V.D., T.T.**; study concepts/study design or data acquisition or data analysis/interpretation, all authors; manuscript drafting or manuscript revision for important intellectual content, all authors; approval of final version of submitted manuscript, all authors; agrees to ensure any questions related to the work are appropriately resolved, all authors; literature research, **H.F., T.Y., I.S., L.C., G.W.A., J.M.O., T.T.**; clinical studies, **H.F., T.Y., I.S., S.C., N.R., J.F.A., L.C., S.S., A.V., P.R., A.G., J.D., A.D., C.T., A.S., F.B., C.C., V.D., J.M.O., T.T.**; statistical analysis, **H.F., T.Y., A.S., V.R.**; and manuscript editing, **H.F., T.Y., I.S., N.R., G.M., S.O., L.C., S.S., A.G., M.P., S.D., M.M., G.W.A., C.C., V.D., J.M.O., T.T.**

**Data sharing:** Data generated or analyzed during the study are available from the corresponding author by request.

**Disclosures of conflicts of interest:** H.F. No relevant relationships. T.Y. No relevant relationships. I.S. Consulting fees and/or lecture payments, Sanofi Synthelabo, Servier, Boehringer Ingelheim, AstraZeneca, Novo Nordisk, Medtronic, and Bristol Myers Squibb—Pfizer. S.C. Stockholder, iSchemaview. N.R. No relevant relationships. G.M. Consulting fees, Stryker Neurovascular and Balt Extrusion; lecture payments, Microvention Europe. J.F.A. No relevant relationships. S.O. No relevant relationships. L.C. Consulting fees, Alexion, AstraZeneca, and Re-Imagine Health Agency; honoraria, Pfizer and Bristol Myers Squibb. S.S. No relevant relationships. A.V. No relevant relationships. P.R. No relevant relationships. A.G. No relevant relationships. M.P. No relevant relationships. J.D. No relevant relationships. S.D. No relevant relationships. A.D. No relevant relationships. C.T. No relevant relationships. A.S. No relevant relationships. V.R. No relevant relationships. M.M. No relevant relationships. F.B. No relevant relationships. G.W.A. Grants, National Institutes of Health; consulting fees, Genentech and iSchemaView; advisory board, Genentech; leadership and stockholder, iSchemaview. C.C. Consulting fees, Stryker, Medtronic, Cerenovus, Mivi, and Microvention. V.D. No relevant relationships. J.M.O. Grants, French Department of Health; consulting fees, AbbVie and Acticor; honoraria, Bristol Myers Squibb; advisory board, Direct Angio and Nets Target. T.T. No relevant relationships.

## References

- Astrup J, Siesjö BK, Symon L. Thresholds in cerebral ischemia - the ischemic penumbra. *Stroke* 1981;12(6):723–725.
- Astrup J, Symon L, Branston NM, Lassen NA. Cortical evoked potential and extracellular K<sup>+</sup> and H<sup>+</sup> at critical levels of brain ischemia. *Stroke* 1977;8(1):51–57.
- Heiss WD. The ischemic penumbra: correlates in imaging and implications for treatment of ischemic stroke. The Johann Jacob Wepfer award 2011. *Cerebrovasc Dis* 2011;32(4):307–320.
- Ma H, Campbell BCV, Parsons MW, et al. Thrombolysis Guided by Perfusion Imaging up to 9 Hours after Onset of Stroke. *N Engl J Med* 2019;380(19):1795–1803 [Published correction appears in *N Engl J Med* 2021;384(13):1278].
- Albers GW, Marks MP, Kemp S, et al. Thrombectomy for Stroke at 6 to 16 Hours with Selection by Perfusion Imaging. *N Engl J Med* 2018;378(8):708–718.
- Olivot JM, Albucher JF, Guenego A, et al. Mismatch Profile Influences Outcome After Mechanical Thrombectomy. *Stroke* 2021;52(1):232–240.
- Campbell BCV, Mitchell PJ, Kleinig TJ, et al. Endovascular therapy for ischemic stroke with perfusion-imaging selection. *N Engl J Med* 2015;372(11):1009–1018.
- Goyal M, Menon BK, van Zwam WH, et al. Endovascular thrombectomy after large-vessel ischaemic stroke: a meta-analysis of individual patient data from five randomised trials. *Lancet* 2016;387(10029):1723–1731.
- Seners P, Oppenheim C, Turc G, et al. Perfusion Imaging and Clinical Outcome in Acute Ischemic Stroke with Large Core. *Ann Neurol* 2021;90(3):417–427.
- Amukotuwa SA, Wu A, Zhou K, Page I, Brotchie P, Bammer R. Distal Medium Vessel Occlusions Can Be Accurately and Rapidly Detected Using *Tmax* Maps. *Stroke* 2021;52(10):3308–3317.
- Kim BJ, Menon BK, Kim JY, et al. Endovascular Treatment After Stroke Due to Large Vessel Occlusion for Patients Presenting Very Late From Time Last Known Well. *JAMA Neurol* 2020;78(1):21–29.
- Marchina S, Zhu LL, Norton A, Zipse L, Wan CY, Schlaug G. Impairment of speech production predicted by lesion load of the left arcuate fasciculus. *Stroke* 2011;42(8):2251–2256.
- Lo R, Gitelman D, Levy R, Hulvershorn J, Parrish T. Identification of critical areas for motor function recovery in chronic stroke subjects using voxel-based lesion symptom mapping. *Neuroimage* 2010;49(1):9–18.
- Cheng B, Forkert ND, Zavaglia M, et al. Influence of stroke infarct location on functional outcome measured by the modified rankin scale. *Stroke* 2014;45(6):1695–1702.
- Magnusdottir S, Fillmore P, den Ouden DB, et al. Damage to left anterior temporal cortex predicts impairment of complex syntactic processing: a lesion-symptom mapping study. *Hum Brain Mapp* 2013;34(10):2715–2723.
- Karnath HO, Rennig J, Johannsen L, Rorden C. The anatomy underlying acute versus chronic spatial neglect: a longitudinal study. *Brain* 2011;134(Pt 3):903–912.
- Wu O, Cloonan L, Mocking S, et al. Role of Acute Lesion Topography in Initial Ischemic Stroke Severity and Long-Term Functional Outcomes. *Stroke* 2015;46(9):2438–2444.
- Munsch F, Sagnier S, Asselineau J, et al. Stroke Location Is an Independent Predictor of Cognitive Outcome. *Stroke* 2016;47(1):66–73.
- Panni P, Michelozzi C, Blanc R, et al. The role of infarct location in patients with DWI-ASPECTS 0–5 acute stroke treated with thrombectomy. *Neurology* 2020;95(24):e3344–e3354.
- Kerleroux B, Benzakoun J, Janot K, et al. Relevance of Brain Regions' Eloquence Assessment in Patients With a Large Ischemic Core Treated With Mechanical Thrombectomy. *Neurology* 2021;97(20):e1975–e1985.
- Coutureau J, Asselineau J, Perez P, et al. Cerebral Small Vessel Disease MRI Features Do Not Improve the Prediction of Stroke Outcome. *Neurology* 2021;96(4):e527–e537.
- Bhatia R, Hill MD, Shobha N, et al. Low rates of acute recanalization with intravenous recombinant tissue plasminogen activator in ischemic stroke: real-world experience and a call for action. *Stroke* 2010;41(10):2254–2258.
- Inoue M, Mlynash M, Straka M, et al. Clinical outcomes strongly associated with the degree of reperfusion achieved in target mismatch patients: pooled data from the Diffusion and Perfusion Imaging Evaluation for Understanding Stroke Evolution studies. *Stroke* 2013;44(7):1885–1890.
- Zhang Y, Kimberg DY, Coslett HB, Schwartz MF, Wang Z. Multivariate lesion-symptom mapping using support vector regression. *Hum Brain Mapp* 2014;35(12):5861–5876.
- Mah YH, Husain M, Rees G, Nachev P. Human brain lesion-deficit inference remapped. *Brain* 2014;137(Pt 9):2522–2531.
- Vigliocco G, Krasan A, Stoll H, Monti A, Buxbaum LJ. Multimodal comprehension in left hemisphere stroke patients. *Cortex* 2020;133:309–327.
- van der Stelt CM, Fama ME, Mccall JD, Snider SF, Turkeltaub PE. Intellectual awareness of naming abilities in people with chronic post-stroke aphasia. *Neuropsychologia* 2021;160:107961.
- Wiesen D, Sperber C, Yourganov G, Rorden C, Karnath HO. Using machine learning-based lesion behavior mapping to identify anatomical networks of cognitive dysfunction: Spatial neglect and attention. *Neuroimage* 2019;201:116000.
- DeMarco AT, Turkeltaub PE. A multivariate lesion symptom mapping toolbox and examination of lesion-volume biases and correction methods in lesion-symptom mapping. *Hum Brain Mapp* 2018;39(11):4169–4182.
- Straka M, Albers GW, Bammer R. Real-time diffusion-perfusion mismatch analysis in acute stroke. *J Magn Reson Imaging* 2010;32(5):1024–1037.
- Avants B, Tustison NJ, Song G. Advanced Normalization Tools: V1.0. *Insight J* 2009.
- Soize S, Fabre G, Gawlitza M, et al. Can early neurological improvement after mechanical thrombectomy be used as a surrogate for final stroke outcome? *J Neurointerv Surg* 2019;11(5):450–454.
- Irvine HJ, Battey TWK, Ostwaldt AC, et al. Early neurological stability predicts adverse outcome after acute ischemic stroke. *Int J Stroke* 2016;11(8):882–889.
- Jamphathong N, Laopaiboon M, Rattanakanokchai S, Pattanittum P. Prognostic models for complete recovery in ischemic stroke: a systematic review and meta-analysis. *BMC Neurol* 2018;18(1):26.
- Kim DE, Park JH, Schellingerhout D, et al. Mapping the Supratentorial Cerebral Arterial Territories Using 1160 Large Artery Infarcts. *JAMA Neurol* 2019;76(1):72–80.
- Senaviratna NAMR, Cooray TMJA. Diagnosing Multicollinearity of Logistic Regression Model. *Asian J Probab Stat* 2019; 1–9.
- Yoshimura S, Sakai N, Yamagami H, et al. Endovascular Therapy for Acute Stroke with a Large Ischemic Region. *N Engl J Med* 2022;386(14):1303–1313.
- Rosso C, Samson Y. The ischemic penumbra: the location rather than the volume of recovery determines outcome. *Curr Opin Neurol* 2014;27(1):35–41.
- Grönholm EO, Roll MC, Horne MA, Sundgren PC, Lindgren AG. Prevalence of caudate nucleus lesions in acute ischaemic stroke patients with impairment in language and speech. *Eur J Neurol* 2016;23(1):148–153.
- Heitsch L, Ibanez L, Carrera C, et al. Early Neurological Change After Ischemic Stroke Is Associated With 90-Day Outcome. *Stroke* 2021;52(1):132–141.
- Requena M, Olivé-Gadea M, Muchada M, et al. Direct to Angiography Suite Without Stopping for Computed Tomography Imaging for Patients With Acute Stroke: A Randomized Clinical Trial. *JAMA Neurol* 2021;78(9):1099–1107.
- Bell CC. DSM-IV: Diagnostic and Statistical Manual of Mental Disorders. *JAMA* 1994;272(10):828–829.